STUDIES ON AG^+ ADSORPTION USING TWO NEW LIGNOCELLULOSIC MATERIALS BASED ON *POPULUS ALBA* L. AND *ROBINIA PSEUDOACACIA* L.

PAUNKA S. VASSILEVA,[*] ALBENA K. DETCHEVA,[*] TEMENUZHKA HR. RADOYKOVA,[**] IVALINA A. AVRAMOVA,[*] KATERINA I. ALEKSIEVA,[***] SANCHI K. NENKOVA,[**] IVO V. VALCHEV[**] and DIMITAR R. MEHANDJIEV[*]

[*]*Institute of General and Inorganic Chemistry, Bulgarian Academy of Sciences, 11, Acad. G. Bonchev Str., 1113 Sofia, Bulgaria*
[**]*University of Chemical Technology and Metallurgy, 8, Kliment Ohridski Blvd., 1756 Sofia, Bulgaria*
[***]*Institute of Catalysis, Bulgarian Academy of Sciences, 11, Acad. G. Bonchev Str., 1113 Sofia, Bulgaria*
✉ *Corresponding author: P.S. Vassileva, pnovachka@svr.igic.bas.bg*

The article is dedicated to the 70th anniversary of Acad. Bogdan C. Simionescu.

The adsorption of Ag^+ ions onto lignocellulosic materials based on two fast-growing tree species *Populus alba L.* (poplar) and *Robinia pseudoacacia L.* (black locust) was studied. Chemical analyses were performed to establish the composition of the obtained materials. Texture parameters were calculated by means of low temperature nitrogen adsorption. The adsorption mechanism was examined using IR, SEM, EPR and XPS spectroscopy. The effects of contact time, acidity and initial Ag^+ ion concentrations were investigated. In both cases, the adsorption was significantly affected by the pH value. Experimental equilibrium data were fitted to the Langmuir, Freundlich and Dubinin-Radushkevich models and the corresponding constants were calculated. The obtained results revealed that the examined waste lignocellulosic materials can be used as adsorbents for Ag^+ ions.

Keywords: adsorption of Ag^+ ions, adsorption equilibrium and mechanism, fast-growing tree species wastes, hydrolyzed lignocellulosic materials

INTRODUCTION

The biomass from plantations of fast-growing tree species, such as willow, poplar, black locust, eucalyptus and paulownia, can be an attractive alternative for bioethanol production.[1-3] Thermochemical pretreatments, such as dilute acid hydrolysis, steam explosion (SE) and hydrothermal pretreatment, which solubilise large parts of the hemicelluloses and thus increase cellulose accessibility, are common preparation steps before lignocelluloses are submitted to enzymatic saccharification.[4-5]

The utilization of waste lignocellulosic materials from bioethanol production is an important task concerning environment protection. One possibility to solve this problem is to investigate the potential to use such materials as low-cost adsorbents or catalysts. By means of waste utilization and conversion into effective sorbents, two environmental problems are solved at once: the expenses for waste storage are reduced, as well as products of practical use are obtained.

Biosorption is an innovative technology aimed at the removal of metal ions from polluted water by using inactive and dead biomasses. Metals entrapment is due to chemicophysical interactions with the active groups present on the cell walls, mostly carboxylic, phosphate, sulphate, amino, amide and hydroxyl groups, depending on the biosorbent nature. An advantage of biosorption is that the biomass used is either an abundant raw material, or a waste from another industrial operation and is cheaply available.[6-10] Another advantage of biosorbents is their biodegradability.

The sorption properties of hydrolyzed lignocellulosic materials towards metal ions are discussed in many publications.[7,9,11-18] Their adsorption is due to the large internal surface area and the availability of different functional groups. According to literature data, the adsorption sites are carboxylic- and phenolic-type surface OH-groups, which form, most probably, coordination bonds between the metal ions and the adjacent chains of the OH-groups in the lignocellulosic components.[12,18]

On the other hand, these biomaterials could be used as carriers of biologically active ions. It can be hence assumed that a lignocellulosic carrier with adsorbed Ag^+ ions on its surface would be a base for preparation of prospective adsorbents for removal of toxic substances from physiologic solutions.

In our previous study,[19] the adsorption of Ag^+ ions onto hydrolyzed plant biomass (willow, paulownia, wheat straw and maize stalks) was investigated. The obtained results revealed that the examined waste lignocellulosic materials are promising adsorbents for Ag^+ ions, as well as for preparation of silver-modified catalytic materials for removal of toxic substances from physiologic solutions.

The subject of the present study is the adsorption of silver ions onto two new lignocellulosic materials based on the fast-growing species *Populus alba* L. (poplar) and *Robinia pseudoacacia* L. (black locust). The investigated materials are by-products resulting from bioethanol production and their utilization will be beneficial from an environmental and economic point of view.

EXPERIMENTAL

Procedures for sample preparation

In the present study, the fast-growing wood species *Populus alba* L. and *Robinia pseudoacacia* L. were used as raw materials: the samples obtained from them were denoted as PA and RP, respectively.

The synthesis of samples PA and RP was performed using steam explosion (SE) treatment for facilitating hydrolysis, followed by enzymatic hydrolysis with cellulase enzyme complex combined with β-glucosidase for acacia and poplar, respectively. SE of wood chips was carried out in a 2 L stainless steel laboratory installation under the following conditions: liquid to solid ratio of 10:1; initial temperature of 100 °C; maximum temperature (*T*max) of 200 °C; pressure of 1.55 MPa; heating time of 60 min, followed by an additional 10 min at *T*max. The residue was washed with distilled water and the obtained hydrolysate was filtered. The solid residue produced in the course of the SE pretreatment was subjected to enzymatic hydrolysis. Enzymatic treatment conditions were as follows: temperature of 50 °C, reaction time of 24 hours, lignocellulosic consistency of 10%, $pH_{initial}$ of 5.5-6.0, pH_{final} of 4.2-4.6 and the cellulase enzyme complex NS22086 with 1000 BHU g^{-1} activity and β-glucosidase NS22118 with 250 CBU g^{-1} activity. Both enzymatic mixtures were provided by Novozymes (Bagsvaerd, Denmark). The enzyme charge of NS22086 was 5%, while that of NS22118 was 0.5% (b.o. dry mass). Enzymatic hydrolysis was carried out in polyethylene bags in a water bath previously heated to the desired temperature. The enzymatic activity was stopped by heating the samples to 100 °C and maintaining that temperature for 10 min.

Sample characterization

The cellulose content in the studied lignocellulosic materials PA and RP was determined according to the procedure described in a previous study,[3] the lignin content – according to TAPPI standard test method T 222 om-11 (Acid-insoluble lignin in wood and pulp), and the ash – according to TAPPI standard T 211 om-02 (Ash in wood, pulp, paper and paperboard: combustion at 525 °C).

An Elemental Analyzer Eurovector EA 3000 was used for analysis of C, N and H. The oxygen content of the samples was calculated by the difference between 100% and the sum of carbon, hydrogen, nitrogen and ash.

The porous structure of the studied materials was investigated by low-temperature (-196 °C) nitrogen adsorption, using a Quantachrome NOVA 1200 apparatus (Quantachrome Instruments, USA). Before nitrogen adsorption, the samples were degassed at 250 °C for 3 h. The specific surface area was calculated on the basis of the Brunauer–Emmett–Teller (BET) equation, whereas the pore size distribution was calculated according to the Barrett-Joyner-Halenda (BJH) method. The total pore volume was estimated in accordance with the rule of Gurvich at a relative pressure of 0.95.

Infrared spectra were measured on a Varian 660 IR spectrometer. Spectra were collected in the mid-infrared region (4000-400 cm^{-1}). Samples were prepared by the standard KBr pellet method.

Scanning electron micrographs (SEM) were obtained on a TESCAN instrument model SEM/FIB LYRA I XMU, using both secondary electron (SE) and back-scattered electron (BSE) detectors.

EPR measurements were performed at room temperature on a JEOL JES-FA 100 spectrometer operated in X-band. A standard cylindrical cavity operating in TE_{011} mode was used. All powder samples were accommodated in quartz EPR sample tubes (i.d./o.d. 4/5 mm) and directly measured.

XPS investigations were carried out by means of an ESCALAB MKII spectrometer with Al Kα (unmonochromatized) source at 1486.6 eV with a total instrumental resolution of ~1 eV, under a base pressure of 10^{-8} mbarr. The C1s, O1s, N1s and Ag3d photoelectron lines were recorded and calibrated to the C1s line at 285.0 eV. All the data were recorded at 45^o take-off angle. The XPSPEAK 4.0 fitting program was used for deconvolution of C1s and O1s photoelectron peaks.

Adsorption studies

A stock standard solution (1000 mg L^{-1}) of Ag^+ ions was prepared (Titrisol, Merck, Germany) and then diluted to obtain the desired pre-set initial concentrations. Adsorption experiments were carried out at 20 ± 1 °C in the batch mode. Experiments were carried out using stoppered 50 mL Erlenmeyer flasks containing about 0.2 g of the investigated sample and 20 mL of the corresponding Ag^+ aqueous solution. The suspensions were shaken on a rotary shaker at 150 rpm. Kinetic adsorption experiments were performed using solutions with initial ion concentrations of 75 mg/L (pH 5.0). The adsorption was investigated at different time intervals, varying from 1 min to 60 min. After reaching equilibrium, the adsorbent was removed by filtration through a Millipore filter (0.2 μm). The initial and equilibrium concentrations of the Ag^+ ions were determined by inductively coupled plasma optical emission spectrometry (ICP-OES) on a Prodigy7 ICP-OES spectrometer (Teledyne Leeman Labs, USA). Measurements were carried out using the Ag II wavelength (243.781 nm, radial viewing) under optimized operating conditions. The calibration solutions were prepared by stepwise dilution of the stock standard solution (Titrisol, Merck, Germany).

The effect of acidity on the adsorption efficiency of the studied samples was investigated over the pH range of 1.0 to 7.0 (pH-meter model pH 211, Hanna Instruments, Germany) at Ag^+ concentration of 75 mg L^{-1}. The pH was adjusted using 0.1 M HNO_3 or 0.1M NaOH. Thus, in order to determine the effect of the initial metal ion concentrations on the adsorption capacity, concentrations in the range of 10-100 mg/L at pH 5.0 were chosen.

Analytical purity grade reagents were used and all adsorption experiments were replicated and the average results were used in the data analyses.

The amount of Ag^+ ions adsorbed onto the investigated samples at equilibrium (Q_e, mg g^{-1}) was calculated using the expression:

$$Q_e = (C_o - C_e) * V/m \quad (1)$$

where C_o and C_e are the initial and equilibrium concentration of Ag^+ (mg L^{-1}), respectively; V is the solution volume (in litres L) and m is the adsorbent weight (g).

Langmuir isotherm

The linear form of the Langmuir isotherm is expressed by the following equation:

$$C_e/Q_e = 1/K_L Q_0 + C_e/Q_0 \quad (2)$$

where C_e is the concentration of metal ions in the equilibrium solution (mg L^{-1}), Q_e is the amount of ions adsorbed (mg) per unit mass of adsorbent (g), Q_0, the maximum adsorption capacity (mg g^{-1}); K_L is the Langmuir constant related to the enthalpy of the process.

The essential characteristics of the Langmuir isotherm can be expressed in terms of a dimensionless constant or separation factor, R_L, which is defined as:

$$R_L = 1/(1 + K_L C_0) \quad (3)$$

The Langmuir model supports the following hypothesis: the adsorbent has a uniform surface, which implies absence of interactions between solid molecules and the fact that the sorption process takes place in a single layer.

Freundlich isotherm

The linear form of the Freundlich model is expressed by the following equation:

$$\ln Q_e = \ln k_F + (1/n) \ln C_e \quad (4)$$

where k_F is a constant related to the adsorption capacity and n is an empirical parameter related to the intensity of adsorption.

The Freundlich model is valid for heterogeneous surfaces and predicts an increase in the concentration of the ionic species adsorbed onto the surface of the solid when increasing the concentration of certain species in the liquid phase.

Dubinin–Radushkevich isotherm

The Dubinin–Radushkevich isotherm reveals the adsorption mechanism based on the potential theory. The linear form of the Dubinin–Radushkevich isotherm is described by the following equation:

$$\ln Q_e = \ln Q_m - \beta\varepsilon^2 \quad (5)$$

where Q_e is the amount of metal ions (mg) adsorbed per unit mass of adsorbent (g), Q_m is the maximum adsorption capacity (mg/g), β is the adsorption energy constant ($mol^2\ J^{-2}$), and ε is the Polanyi potential, described as:

$$\varepsilon = RT \ln(1+1/C_e) \quad (6)$$

where R is the gas constant (J $mol^{-1}K^{-1}$) and T is the temperature (K). The mean adsorption energy E (KJ mol^{-1}) can be calculated using the parameter β as follows:

$$E = 1/(-2\beta)^{1/2} \quad (7)$$

RESULTS AND DISCUSSION

The chemical composition of the investigated materials is presented in Table 1. Concerning the composition of the waste lignocellulosic mass after enzymatic hydrolysis, only the amounts of cellulose and lignin are determined, because it is assumed that the hemicelluloses are practically hydrolyzed. This is also evidenced by the amounts of cellulose and lignin, the sum of which, in each species, is over 99% (see Table 1). The studied materials RP and PA contain lignin and polysaccharides, strongly connected to the former and resistant to hydrolysis. The data show that the samples do not differ substantially as regards their elemental composition. The material based on poplar (RP) has higher cellulose content and lower lignin content (lower extent of hydrolysis), as compared to the sample based on black locust PA.

The nitrogen adsorption-desorption isotherms and the pore size distribution of the investigated materials are presented in Figure 1. Both isotherms belong to type IV, with a hysteresis loop, resembling the H3 type in the IUPAC classification. This hysteresis pattern can be attributed to the crystalline agglomerates that result in the mesoporous structure formed by the interparticle space that causes formation of secondary pores.[21] The porosity diagrams are of analogous appearance, which shows that both materials possess pores of similar dimensions. There are two kinds of pores: some are in the range of 15-20 nm and the others have a diameter of about 3 nm. The textural parameters of RP and PA are summarized in Table 2. The sample RP displays slightly higher values for the specific surface area and total pore volume. The calculated average pore diameters are 17 nm (PA) and 20 nm (RP) corresponding to a mesoporous structure.

Table 1
Chemical composition of the investigated hydrolyzed materials

Sample	Chemical composition			Elemental composition			
	Mineral substances (%)	Cellulose (%)	Lignin (%)	C (%)	H (%)	N (%)	O (%)
PA	0.1	40.7	59.1	53.6	6.0	1.0	39.3
RP	0.2	48.0	51.3	53.2	6.0	1.0	39.6

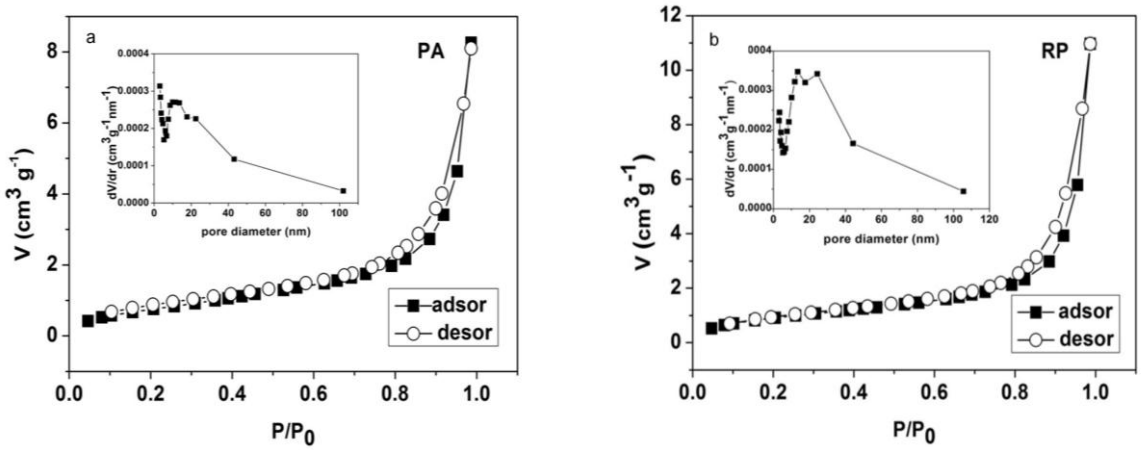

Figure 1: Nitrogen adsorption-desorption isotherms and pore size distribution of PA (a) and RP (b)

Table 2
Texture parameters of the investigated hydrolyzed materials

Sample	S ($m^2 g^{-1}$)	V_t ($cm^3 g^{-1}$)	Average pore size (nm)
PA	3.0	0.013	17
RP	3.5	0.017	20

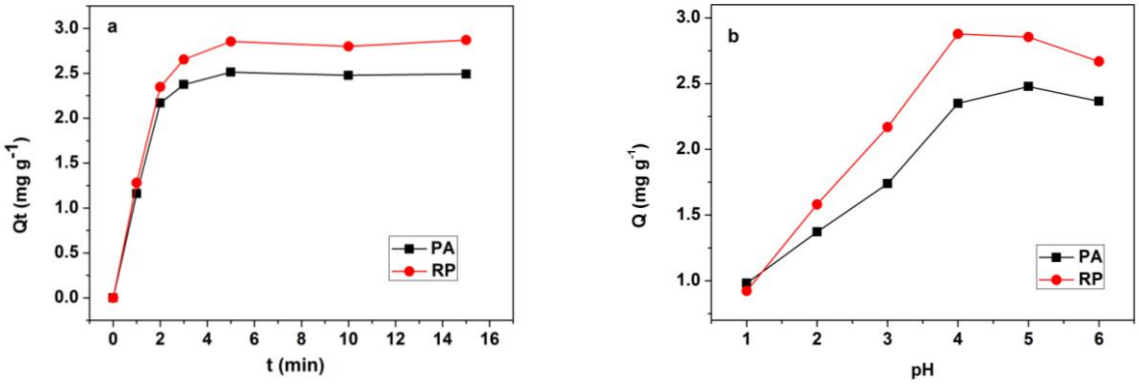

Figure 2: Effect of contact time (a) and acidity (b) on the amount of Ag^+ ions adsorbed onto the investigated materials RP and PA

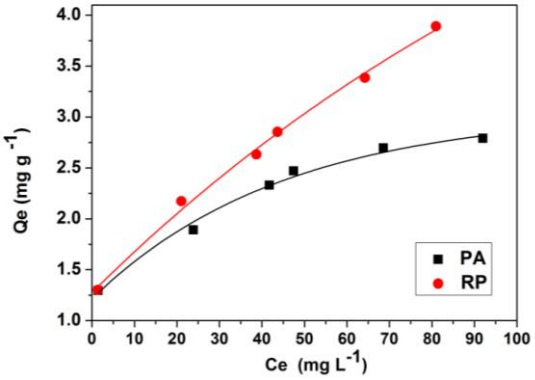

Figure 3: Adsorption isotherms of Ag^+ ions onto the investigated materials RP and PA

Figure 2a shows the effect of contact time on the Ag^+ adsorption onto both materials. It is evident that the sorption capacity increases with an increase in contact time. It has been found that equilibrium is attained after about 4-5 min. This short time required to reach equilibrium implies an excellent affinity of the studied materials toward silver ions. Nevertheless, all further experiments were performed at a contact time of 30 min for certainty.

Figure 2b shows the effect of acidity on the Ag^+ adsorption onto both materials. With the increase in pH, the amount of adsorbed ions increases and the optimal pH value has been found to be in the range of about 4-5. It is known that the increase in pH decreases the competition between the hydroxonium and metal ions for surface sites and results in increased uptake of metal ions by the adsorbents. The increase in metal uptake by adsorbents of different types, due to increasing solution pH, has been reported in our previous studies.[19-24]

At a pH of about 6, a slight degree of opalescence is observed, which is the explanation for the slight decline in the adsorbed amount of Ag^+ ions (Fig. 2b). At pH 7, and above hydrolysis of Ag occurs. Therefore, the study on the effect of pH values beyond 7 was excluded, because insoluble silver hydroxide precipitate was formed, which is in accordance with literature data.[25]

Adsorption isotherms obtained under equilibrium conditions are very important in designing adsorption systems, since such isotherms describe the distribution of adsorbed molecules between the liquid and solid phases in the equilibrium state. Concentration variation methods are normally used to calculate the adsorption characteristics of adsorbents and processes, with the elucidation of isotherm data by fitting them to different isotherm models. The experimental adsorption isotherms are presented in Figure 3. In the present study, the equilibrium data were analyzed using the Langmuir, Freundlich and Dubinin–Radushkevich isotherm models. The corresponding parameters calculated from their linear plots are given in Table 3.

Table 3
Langmuir, Freundlich and Dubinin–Radushkevich parameters for Ag^{+} adsorption

Sample	Langmuir parameters			Freundlich parameters			Dubinin–Radushkevich parameters		
	Q_o (mg g^{-1})	K_L (L mg^{-1})	r^2	k_F ($mg^{1-n}L^n g^{-1}$)	n (L mg^{-1})	r^2	Q_o (mg g^{-1})	E (KJ mol^{-1})	r^2
PA	2.93	0.119	0.9898	1.17	5.53	0.9382	2.33	1.17	0.6964
RP	4.18	0.070	0.9063	1.13	4.02	0.9817	2.83	1.05	0.6473

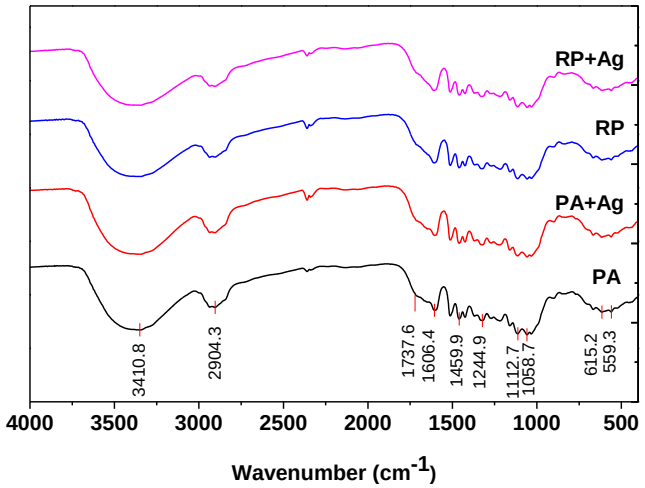

Figure 4: Infrared spectra of RP and PA samples before and after silver adsorption

The Langmuir, Freundlich and Dubinin–Radushkevich equations are based on entirely different principles and the fact that the experimental results fit to one or another equation indicates only a purely mathematical fit. It is important to note that every model has its own limitations in accurately describing equilibrium data.

According to the correlation coefficient for the Dubinin–Radushkevich equation r^2 (values from 0.6964 to 0.6473, Table 3), the fit of this model is worse than those of the other two models.

From the data listed in Table 3, we consider that the mechanism of adsorption of silver ions onto both materials cannot be attributed directly to the Langmuir or Freundlich models (the r^2 values suggest that both isotherm models provide a good correlation). From the linear Langmuir model, the maximum adsorption capacities for silver ions were calculated. Higher adsorption capacity is achieved with the material RP. The adsorption properties depend on many factors defined by the textural and surface parameters. Obviously, the higher adsorption capacity of the RP sample was mainly due to the higher total pore volume and higher specific surface area of this material. Nevertheless, both materials could be used as effective adsorbents for Ag^+ ions from aqueous solutions. The lignocellulosic materials in the present study with incorporated silver will be later investigated for their antibacterial activity and their potential application in microbial infections and therapy.

The Langmuir parameters can be used to predict the affinity between the sorbate and sorbent using the dimensionless separation factor R_L. The R_L values are found to vary within the ranges: 0.078-0.456 (for sample PA) and 0.588-0.125 (for sample RP). All the values are in the range of 0-1, which indicates favorable adsorption for both biomaterials. In addition, the values of the separation factor (R_L) prove that waste lignocellulosic materials are potential sorbents for siver ions from aqueous solutions.

The IR spectral data for samples RP and PA before and after adsorption of Ag^+ ions are presented in Figure 4. In the IR spectrum of both materials, clearly defined bands are observed, which are typical of the functional groups of the components of lignocellulosic materials[18,26] as follows: at about 3411 cm^{-1} – OH-groups of cellulose and lignin; at 2904cm^{-1} – stretching vibrations of C-H bonds in methyl and methylene groups; at 1738 cm^{-1} – vibrations of C=O bonds. A well-formed band is observed at 1245 cm^{-1} and is related to skeleton vibrations of the aromatic rings. Other bands that appear in the spectra of almost all lignins are at 1600 and 1510 cm^{-1}, the latter being usually stronger. These bands are connected with valent oscillations of C-C bonds in the aromatic nucleus of lignin. It is thought that the bands at 1460 cm^{-1} are related to CH_2 deformation vibrations in lignin.

The band at 1059 cm^{-1} refers to C=O valent oscillations and that at 1113 cm^{-1} – to -OH bands in the cellulose. The presence of different functional groups, such as -OH, COOH, -C-O-C- *etc*., makes the shape of spectral bands broader and more complex, due to the hydrogen bonds and conformational structure of the materials. The shape and shifting of the bands before and after silver adsorption onto both materials have not changed considerably.

Figure 5 shows the scanning electron microscopy (SEM) images for both investigated samples RP and PA, before (a, c) and after (b, d) adsorption of silver ions, respectively. As shown in Figure 5 (a) and (c), many pores and particles are present on the surface of raw RP and PA. Also, the electron dense part, which is thought to be silver adsorption, is noted in Figure 5 (b) and (d), as compared with (a) and (c). In Figure 5 (b) and (d), the pores of both materials are partially covered with small bright Ag particles (as reported in[27]) with the diameter <0.5 μm.

As may be remarked from the EPR spectra (Fig. 6), a narrow singlet line with g factor of 2.0026 is recorded, which is due to Ag^0.[28] In addition, EPR lines are detected at g factors of 4.0912 and 2.1833, attributed to Fe^{3+} ions in tetragonal and octahedral environment, respectively.[19] Ag^+ ion is diamagnetic with filled-up $4d^{10}$ electronic configuration, and it does not exhibit any EPR spectrum. Some of the silver species are paramagnetic: Ag^0 (with the $4d^{10}5s^1$ electronic configuration), Ag^{2+} (with the $4d^9$ electronic configuration), as well as some silver clusters. The g factor of Ag^0 is reported to be isotropic and close to the free electron value of 2.0023, while signals attributed to Ag^{2+} occur at $g_I \approx 2.05$ and $g_{II} \approx 2.35$. Aggregation of Ag^0 and Ag^+ ions may additionally generate chemically stable Ag_y^{x+} clusters, such as Ag_2^+, Ag_3^{2+}.[19,29]

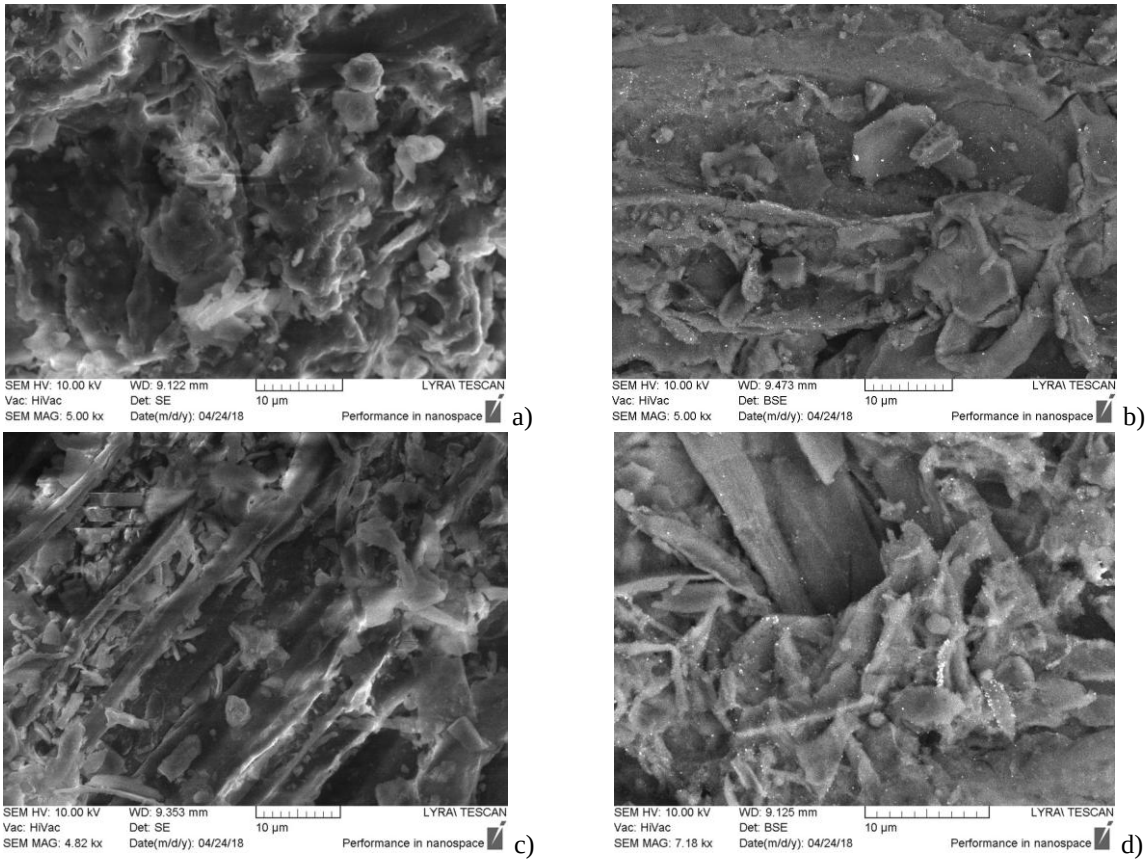

Figure 5: SEM images of RP and PA samples before (a, c) and after (b, d) silver adsorption

Table 4
Atomic surface concentrations of constituent elements and carbon functional groups present on the surface of the studied samples

Sample	C (at.%)	O (at.%)	N (at.%)	Ag (at.%)	C1, C-C	C2, C-O or/and OH	C3, C=O	C4, O-C=O
PA	71.61	27.06	1.33	-	50.96	39.50	9.44	-
PA+Ag	62.74	34.69	2.47	0.09	50.28	41.70	8.00	-
RP	76.94	21.80	1.26	-	51.22	39.34	9.43	-
RP+Ag	60.76	36.2	2.78	0.25	49.00	38.06	12.56	0.36

It follows from the obtained results that the adsorption of silver ions on both samples takes place through a complex mechanism (involving physical sorption, chelating and ion-exchange), in which the phases are defined silver clusters of Ag_y^{x+} type and clusters of metallic silver are formed as a final phase in the investigated samples, as observed in our previous study.[19]

The atomic surface concentrations of constituent elements in the studied samples, as well as the calculated amounts of carbon functional groups present on the surface of both waste lignocellulosic materials before and after adsorption of Ag^+ ions are presented in Table 4.

Higher surface Ag concentration was calculated for the sample RP, which is in accordance with the data obtained for the adsorption capacities (Table 3). For both untreated materials, the presence of nitrogen is almost equal and doubled after Ag treatment.

The high resolution C1s photoelectron lines recorded for the samples examined by us have been fitted by three components named C1, C2 and C3, respectively, and related to different existing bonds on their surfaces. The first C1 (peak at ≈ 285 eV) component is associated to C-C/C-H bonds, the C2 (peak at ≈ 286.5 eV) component corresponds to the existence of C-O-C/C-OH bonds, the C3 (peak at ≈ 288.0 eV) component belongs to C=O bonds, and the last C4 (peak at 289.5 eV) corresponds to the O–C=O bond.

The O1s peak shows two components: at 532.0 and 533.5 eV, which fit the O1s peaks for both studied adsorbents. The two components can be assigned to the existence of organic groups, such as C=O and C–O/C–OH, respectively, but not to Ag_2O (528.5-529.3 eV) or AgO (529.2-530.9 eV).

The Ag3d photoelectron line was also detected (Fig. 7). Ferraria *et al.*[30] specify how to distinguish the silver in different oxidation states. Taking their investigations into account and having in mind the loading procedure of silver onto both materials in the present study, most probably in this case the chemical state of silver is Ag(0), although the evaluated binding energy is a little bit higher than that reported in the literature.[31]

The XPS and EPR results confirm the complex character of the adsorption of Ag^+ ions onto the hydrolyzed lignocellulosic waste materials, and they prove the formation of metallic Ag clusters on the surface of both studied materials. According to the obtained results, the adsorption of Ag^+ ions passes through several stages. The final stage (EPR and XPS results) is the formation of Ag^0 as follows:

Ag+ (solution) ---- Ag+ (adsorbate) ---- Ag_y^{n+} (adsorbate) ---- Ag^o (adsorbate) (8)

Hence, we confirm the adsorption mechanism, which was also observed when using lignocellulosic materials based on willow, paulownia, wheat straw and maize stalks.[19]

Figure 6: EPR spectra of RP (a) and PA (b) samples after silver adsorption

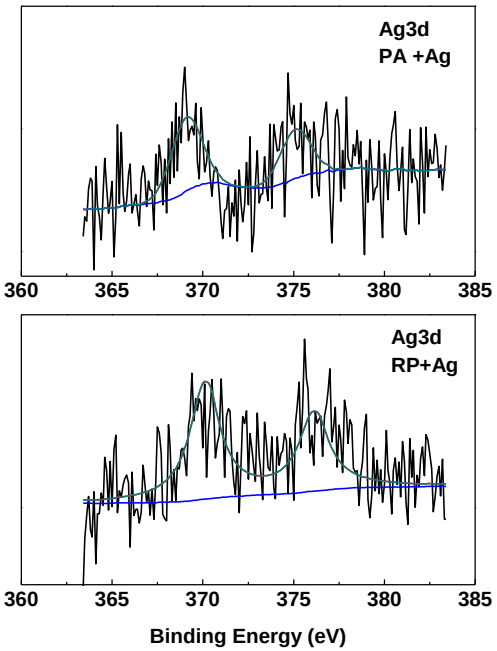

Figure 7: Photoelectron core level of lignocellulosic waste materials after adsorption of Ag ions for Ag3d

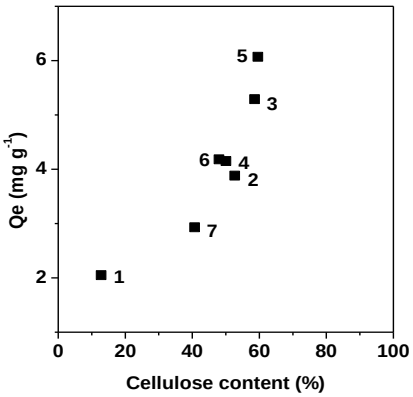

Figure 8: Adsorption capacities *vs*. cellulose content for the investigated materials based on: 1 – technical hydrolyzed lignin, 2 – willow, 3 – paulownia, 4 – wheat straw, 5 – maize stalks (Ref. 19), 6 – black locust and 7 – poplar (the present study)

Combining the results from our previous study[19] and the present investigation, it is observed that the amounts of adsorbed silver on the investigated materials increase with the increase of cellulose content (Fig. 8). This is in agreement with Hanzlík *et al*.[32] It should be mentioned that this is only a trend, because the values for the adsorption capacities are calculated using the Langmuir model equation, as in all the cases the correlation coefficients r^2 are lower than 1.

CONCLUSION

In the present work, the adsorption of Ag^+ ions onto two new hydrolyzed lignocellulosic materials was studied. The investigated materials are by-products obtained from bioethanol production and their utilization will represent a significant contribution from the environmental and economic point of view.

The influence of the acidity of the initial metal ion solutions on their adsorption was investigated, and the optimal pH value was found out to be in the range of about 4-5. The adsorption equilibrium was established within 5 min.

Both Langmuir and Freundlich types of isotherms describe the adsorption process. The adsorption mechanism was investigated, and it was proved that the adsorption of Ag^+ ions passes through several stages. The final stage is the formation of metallic Ag^0. The investigated materials could be used as adsorbents for Ag^+ ions, as well as for the preparation of silver-modified materials with antimicrobial properties. Combining previous results with those obtained in the present work, it is observed that the amounts of adsorbed silver onto all the investigated lignocellulosic materials increase with the increase of the cellulose content. The lignocellulosic waste materials examined in the present study, with incorporated silver, will be later investigated with regard to their antibacterial activity and their potential application in microbial infections and therapy.

REFERENCES

1 F. Schűtt, J. Puls and B. Saake, *Holzforschung*, **65**, 453 (2011).
2 S. González-García, M. T. Moreira, G. Feijoo and R. J. Murphy, *Biomass Bioenerg*., **39**, 378 (2012).
3 I. Valchev, N. Yavorov and S. Petrin, *Holzforschung*, **70**, 1147 (2016).
4 W. El-Zawawy, M. Ibrahim, Y. Abdel-Fattah, N. Soliman and M. Mahmoud, *Carbohyd*. *Polym*., **84**, 865 (2011).
5 J. F. García, S. Sanchez, V. Bravo, M. Cuevas, L. Rigal *et al*., *Holzforschung*, **65**, 59 (2011).
6 B. Volesky, *Hydrometallurgy*, **59**, 203 (2001).
7 J. L. Gardea-Torresdey, G. De La Rosa and J. R. Peralta-Videa, *Pure Appl. Chem*., **76**, 801 (2004).
8 N. T. Abdel-Ghani, M. Hefny and G. A. F. El-Chaghaby, *Int*. *J*. *Environ*. *Sci*. *Tech*., **4**, 67 (2007)
9 K. Krishnani, X. Meng and L. Dupont, *J. Environ*. *Sci*. *Health A*, **44**, 688 (2009).
10 X. Liu, H. Zhu, C. Qin, J. Zhou, J. R. Zhao *et al*., *Bioresourses*, **8**, 2257 (2013).
11 K. Flogeac, E. Guillon, E. Marceau and M. Aplincourt, *New J. Chem*., **27**, 714 (2003).
12 X. Guo, S. Zhang and X. Shan, *J. Hazard*. *Mater*., **151**, 134 (2008).
13 G. Harman, R. Patrick and T. Spittler, *Ind. Biotechnol*., **3**, 366 (2008).
14 N. Tazrouti and M. Amrani, *Bioresources*, **4**, 740 (2009).

[15] C. Bumba, E. P. Leonte, C. Dumitrescu, I. Ghita and M. Stefanescu, *J. Environ. Prot. Ecol.*, **11**, 822 (2010).
[16] J.-G. Cao, X.-M. Li, Y. Ouyang, W. Zheng and Q. Yang, *J. Environ. Prot. Ecol.*, **12**, 661 (2011).
[17] I. H. Bukhari, G. Shabbir, J. Rehman, M. Riaz, N. Rasool *et al.*, *J. Environ. Prot. Ecol.*, **14**, 453 (2013).
[18] T. Radoykova, S. Dimitrova, I. Aleksieva, S. Nenkova, I. Valchev *et al.*, *J. Environ. Prot. Ecol.*, **16**, 23 (2015).
[19] P. S. Vassileva, T. Hr. Radoykova, A. K. Detcheva, I. A. Avramova, K. I. Aleksieva *et al.*, *Int. J. Environ. Sci. Technol.*, **13**, 1319 (2016).
[20] P. Vassileva, A. Detcheva, S. Uzunova, I. Uzunov and D. Voykova, *Separ. Sci. Technol.*, **51**, 797 (2016).
[21] P. Vassileva and A. Detcheva, *Adsorpt. Sci. Technol.*, **28**, 229 (2010).
[22] P. Vassileva and A. Detcheva, *Int. J. Coal Prep. Util.*, **31**, 242 (2011).
[23] P. Vassileva, A. Detcheva, R. Georgieva, D. Voykova, T. Gerganova *et al.*, *Cent. Eur. J. Chem.*, **9**, 932 (2011).
[24] P. Vassileva, A. Detcheva, L. Ivanova and S. Evtimova, *Compt. Rend. Acad. Bulg. Sci.*, **70**, 497 (2017).
[25] C. Jeon, *Korean J. Chem. Eng.*, **34**, 384 (2017).
[26] K. Nakamoto, in "Infrared Spectra of Inorganic and Coordination Compounds", 2nd ed., Wiley, New York, 1970.
[27] M. Yurtsever and A. Sengil, *Trans. Nonferrous Met. Soc. China*, **22**, 2846 (2012).
[28] B. Dhabekar, S. Menon, E. A. Raja, S. S. Sanaye, T. K. G. Rao *et al.*, *J. Phys. D*, **39**, 488 (2006).
[29] A. Baldansuren and E. Roduner, *Chem. Phys. Lett.*, **473**, 135 (2009).
[30] A. M. Ferraria, A. P. Carapeto and A. M. Botelho do Rego, *Vacuum*, **86**, 1988 (2012).
[31] I. Herrera, J. L. Gardea-Torresdey, K. J. Tiemann, J. R. Peralta-Videa, V. Armendariz *et al.*, *J. Hazard. Subst. Res.*, **4**, 1 (2003).
[32] P. Hanzlík, J. Jehlička, Z. Weishauptová and O. Šebek, *Plant Soil Environ.*, **50**, 257 (2004).